Electronic Supplementary Information

Vat photopolymerization using catalytic chain transfer polymerization (CCTP) derived reactive oligomer to improve the mechanical properties

Wai Hin Lee[a], Zhongyuan Wan[b], Ataulla Shegiwal[a], David Haddleton[a],[b]*

[a]: Halcyon3D Ltd., 27f Ignite House, Venture Centre, Coventry, CV4 7EZ,

[b]: Department of Chemistry, University of Warwick, Coventry, CV4 7AL

Email: a.shegiwal@halcyon3d.co.uk, D.M.Haddleton@warwick.ac.uk

Figures

Tables

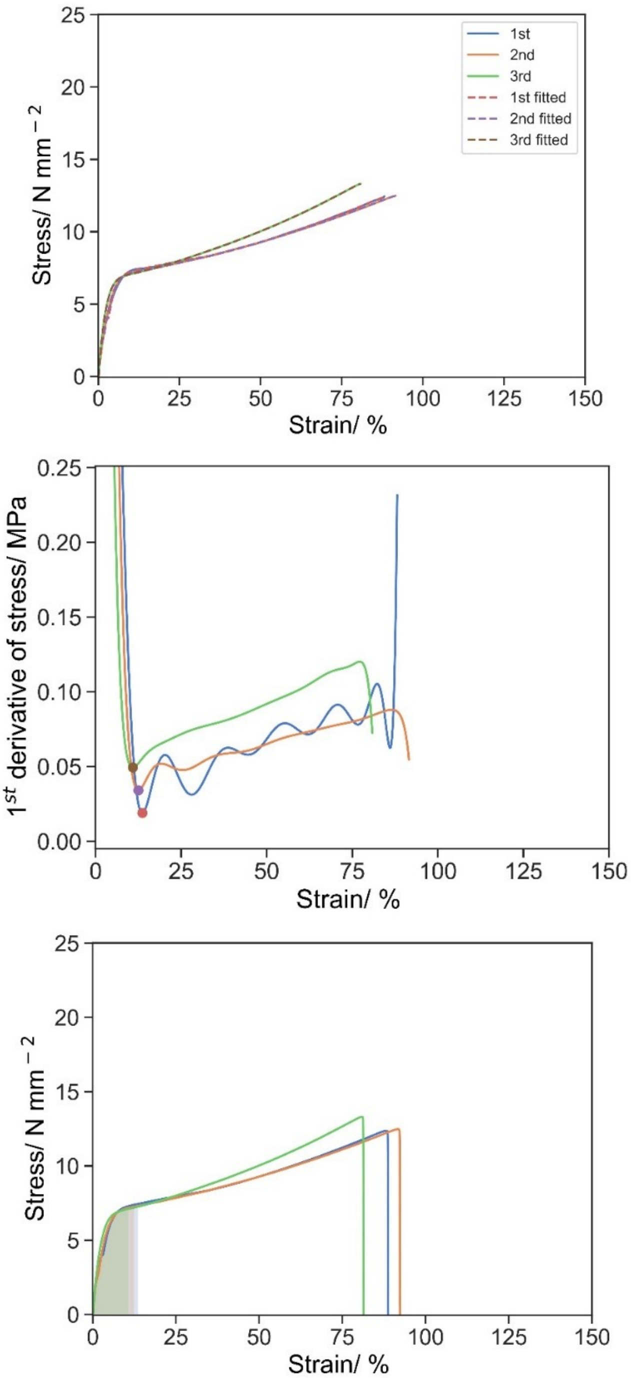

Figure S.1 Determination of knee point by 15th order polynomial fit, then finding the minimum 1st derivative and its integration to the knee point from stress-strain curves by tensile test.

An example of 15th order polynomial fitting of stress strain curve and the determination of knee point at the minimum first derivative of the fitted curve; and the derived specific deformation energy by the integration to the knee point (shaded area).

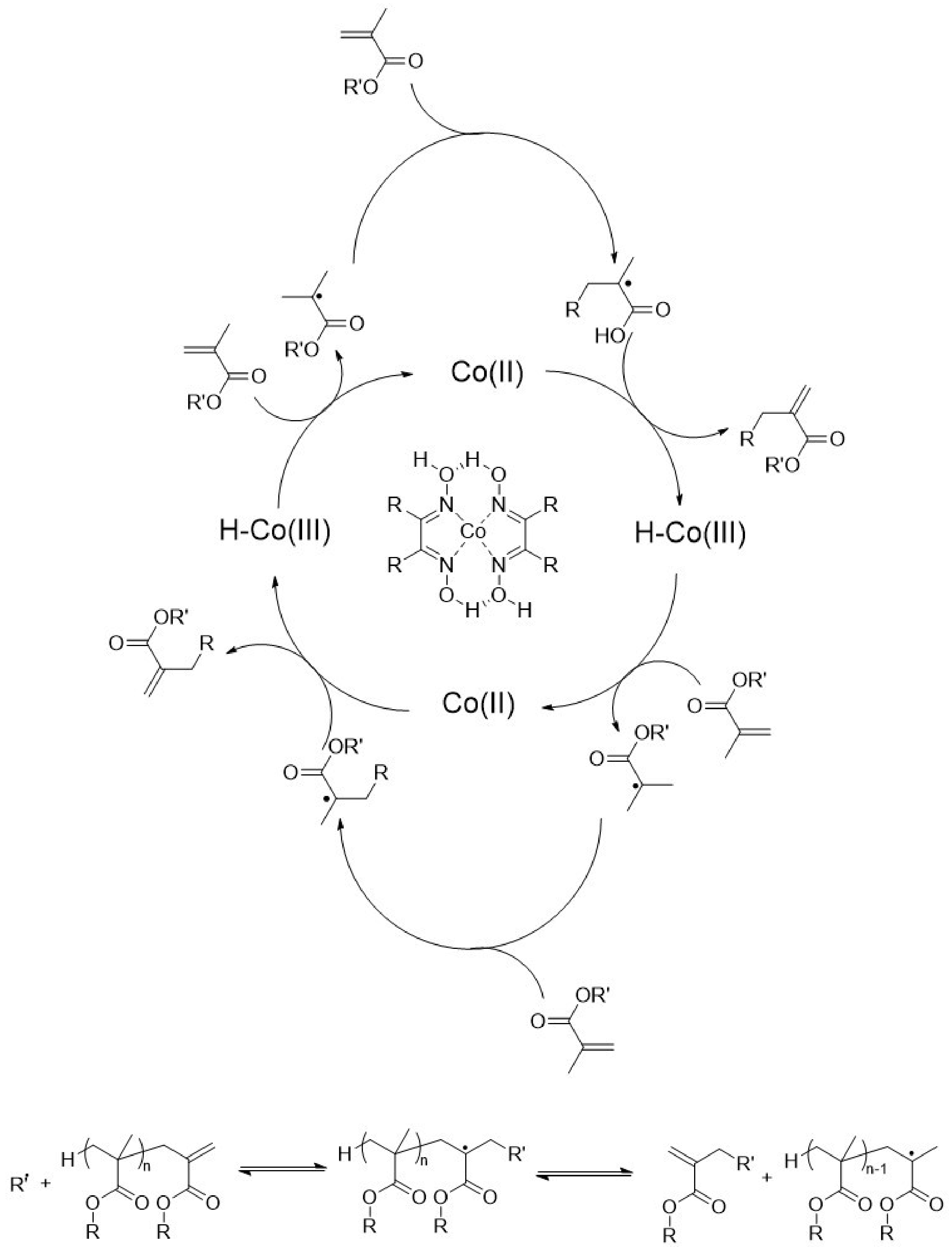

Figure S. 2 Mechanism of CCTP to synthesize ω-vinyl terminated oligomers and AFCT mediated by the derived ω-vinyl terminated oligomers

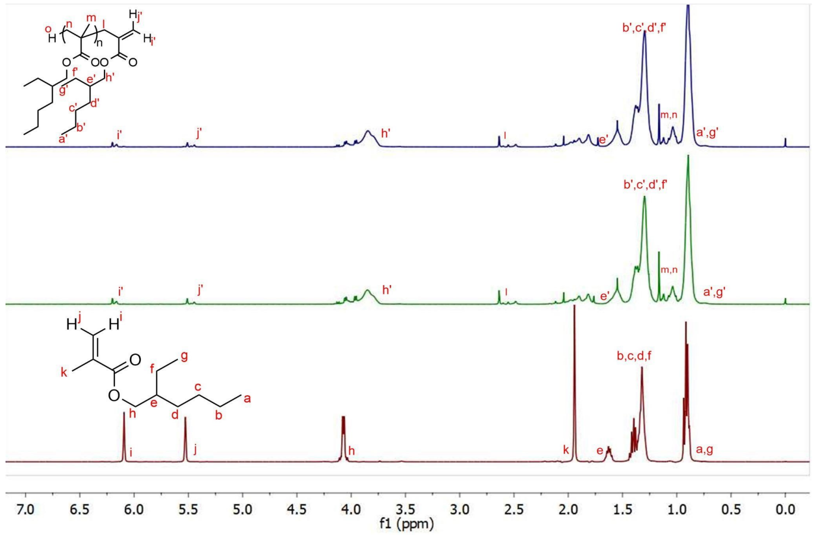

Figure S 3 ^{1}H NMR ($CDCl_3$, 400 MHz) spectra of EHMA monomer (red, bottom), $EHMA_5$ (green, middle) and $EHMA_{15}$ (blue, top) reactive oligomer synthesized via CCTP and subsequent AFCT

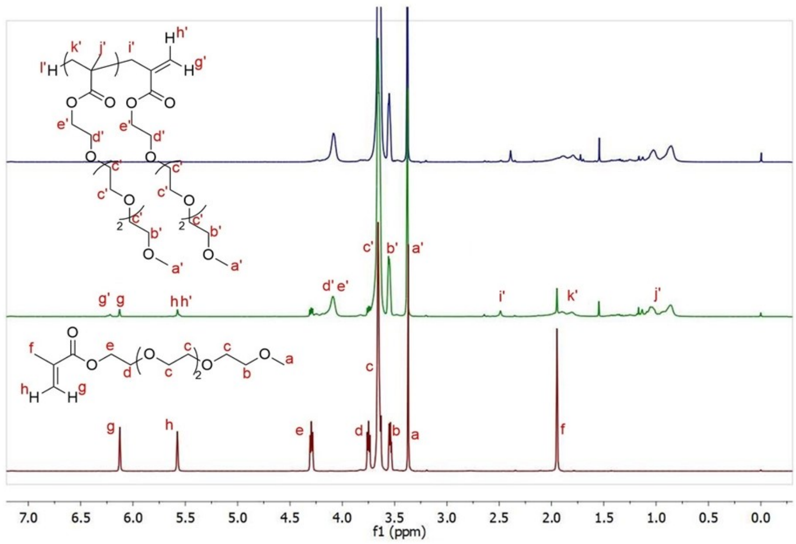

Figure S 4 ^{1}H NMR spectra ($CDCl_3$, 400 MHz) of PEGMA monomer (red, bottom), $PEGMA_{14}$ (green, middle) and $PEGMA_{28}$ (blue, top) reactive oligomer synthesized via CCTP and subsequent AFCT

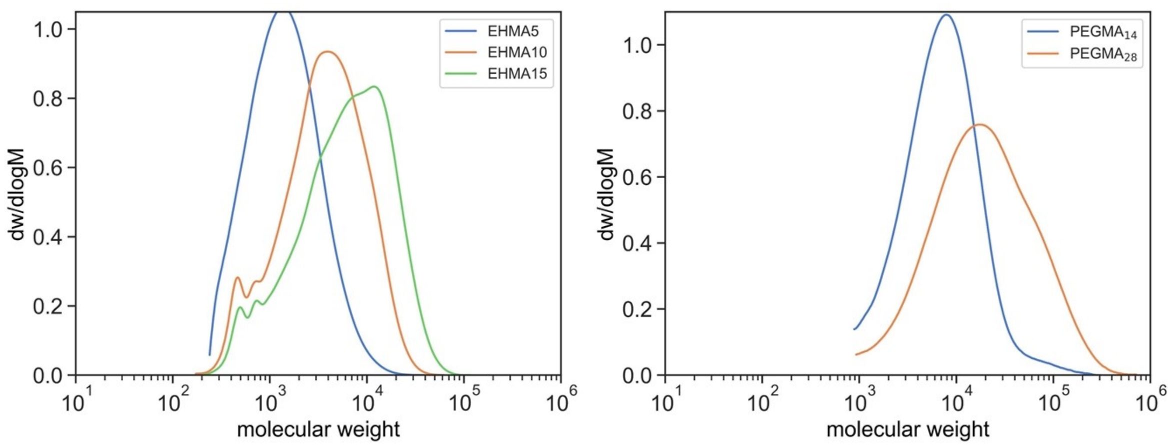

Figure S 5 Molecular weight distribution (left): $EHMA_5$ reactive oligomer via CCTP (blue), and $EHMA_{10}$ (orange) $EHMA_{15}$ (green) reactive oligomer via subsequent AFCT; and (right): $PEGMA_{14}$ (blue) and $PEGMA_{28}$ (orange) via subsequent AFCT.

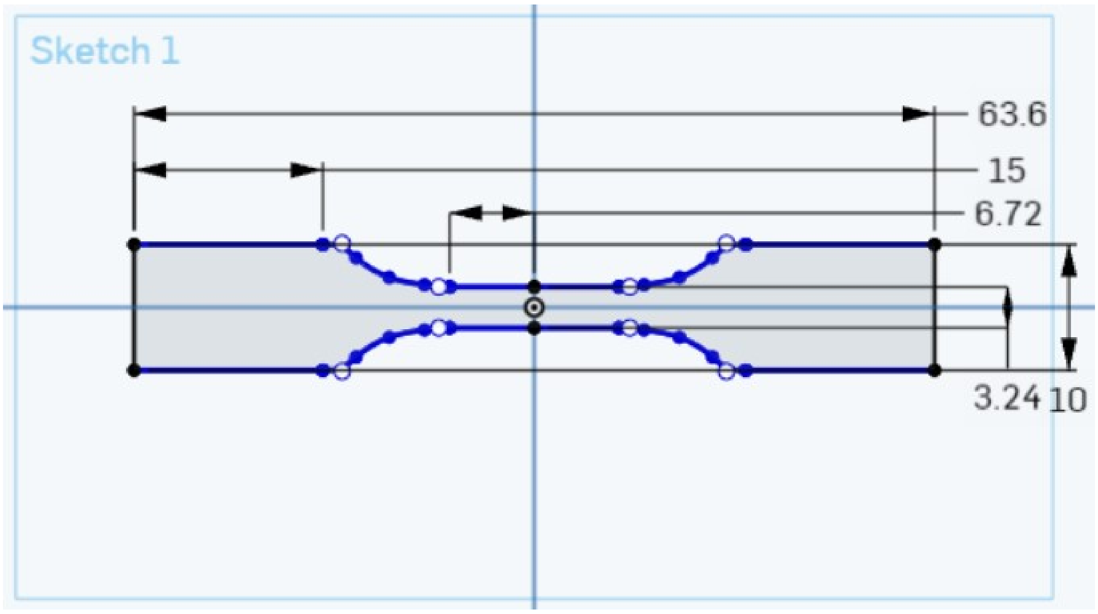

Figure S.6 .stl model of dogbone specimen for mechanical testing. All values are in mm with the thickness of 3 mm from the top, and typical photo of as-printed parts

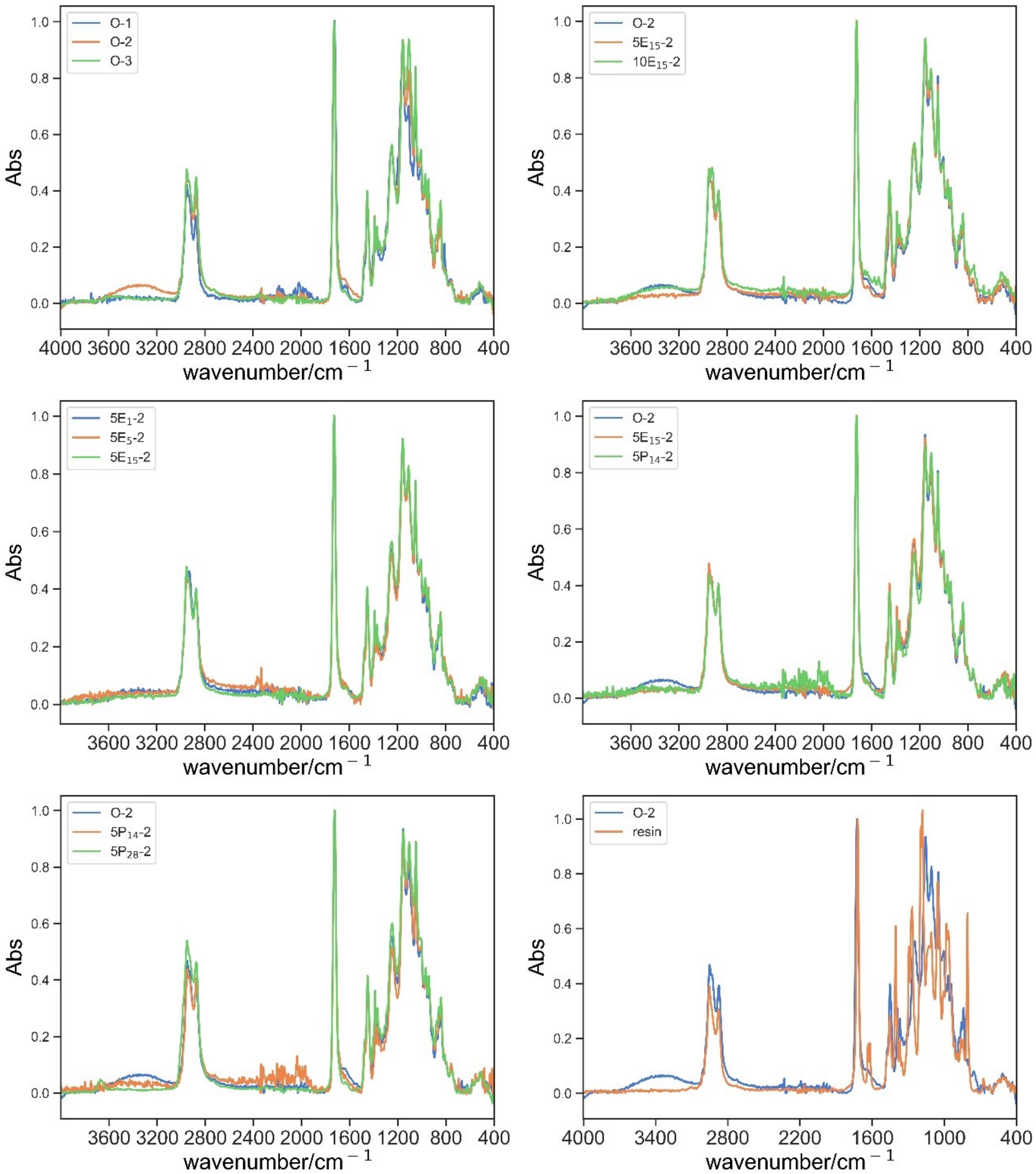

Figure S7 FTIR spectra of 3D printed parts and the original resin. The disappearance of the band at 816 and 1636 cm-1 of the acrylic $=CH_2$ and C=C suggests the high conversion of the printed parts.

Table S. 1 IR bands and their assignment of the 3D printed parts

Wavenumber/ cm^{-1}	Assignments	Ref.
2951	Asym C-H stretch (CH_3)	[1]
2876	Sym C-H stretch (CH_3)	[2]
1724	C=O stretching	[2]
1452	C-H def.	[1]
1391	C-(CH_3) sym def.	[3]
1371	C-(CH_3) sym def.	[2]
1248	-C-C-O stretching	[4]
1159	C-O-C stretching	[3]
1110	Sym C-O-C stretch	[4]
1051	Sym C-O-C stretch	[3]
969	CH_2-O (ether)	[2]
942	CH_2-O (ether)	[2]
816	=C-H out-of-plan	[4]

Table S. 2 Stress (σ), strain (ε) and specific energy (U_T) at knee point ($_K$) and the ultimate point ($_U$) of printed parts measured by tensile testing at 50 mm s^{-1}

Sample	σ_K/ MPa	ε_K/ %	$U_{T,K}$/ MPa	σ_U/ MPa	ε_U/ %	$U_{T,U}$/ MPa
O-1	45.71 (1.48)	17.03 (1.04)	443.51 (34.91)	44.39 (1.39)	18.14 (1.72)	502.30 (66.97)
O-2	26.78 (0.54)	8.10 (0.57)	136.62 (14.59)	18.87 (1.02)	21.13 (1.31)	415.97 (15.42)
O-3	7.28 (0.13)	12.34 (1.13)	70.96 (5.58)	12.64 (0.43)	87.68 (4.59)	796.94 (32.40)
10-E_{15}-1	20.58 (0.66)	6.53 (0.43)	77.92 (6.28)	20.16 (0.47)	6.57 (0.43)	80.55 (6.40)
10-E_{15}-2	13.44 (0.66)	8.17 (0.45)	73.77 (6.52)	12.82 (0.61)	8.86 (0.87)	83.67 (9.23)
10-E_{15}-3	6.38 (0.42)	22.78 (0.36)	114.03 (7.76)	11.07 (0.78)	84.16 (5.91)	644.54 (85.60)
5-E_1-2	23.88 (0.90)	8.44 (0.29)	126.81 (3.69)	19.01 (0.64)	34.21 (1.78)	635.06 (35.42)
5-E_5-2	21.93 (0.97)	8.12 (1.52)	112.04 (13.79)	17.85 (0.77)	17.92 (5.03)	302.25 (74.75)
5-E_{15}-2	19.31 (1.07)	8.13 (1.06)	101.90 (17.63)	15.76 (0.41)	25.77 (3.98)	400.31 (51.48)
5-P_{14}-2	17.61 (1.11)	8.06 (1.46)	95.10 (21.48)	16.47 (0.77)	39.61 (4.41)	609.65 (52.25)
10-P_1-2	7.65 (0.18)	21.17 (1.88)	102.26 (8.90)	11.23 (1.29)	71.69 (1.68)	615.18 (9.98)
10-P_{14}-2	13.76 (0.37)	9.93 (1.44)	95.61 (12.66)	14.06 (0.96)	38.79 (1.46)	495.59 (11.54)
10-P_{28}-2	17.10 (0.40)	9.35 (0.88)	109.27 (10.74)	15.08 (0.34)	30.37 (2.66)	442.10 (35.03)

Table S. 3 Temperature at maximum tan δ ($T_{max\ tan\ \delta}$) and the peak width at 25% ($\delta T_{25\%}$), 50% ($\delta T_{50\%}$), and 75% ($\delta T_{75\%}$) height

Sample	$T_{max\ tan\ \delta}$	$\delta T_{25\%}$	$\delta T_{50\%}$	$\delta T_{75\%}$
O-1	74.1	17.2	11.4	7.2
O-2	61.8	18.3	11.8	7.0
O-3	44.0	23.9	14.6	8.6
$10E_{15}$-1	70.1	15.6	9.2	5.1
$10E_{15}$-2	55.1	33.4	19.5	9.3
$10E_{15}$-3	35.7	25.8	16.0	9.7
$5E_1$-2	53.8	19.3	10.4	5.0
$5E_5$-2	54.6	20.2	9.7	4.8
$5E_{15}$-2	57.8	22.7	12.1	6.7
$5P_{14}$-2	60.1	25.0	15.2	9.4
$10P_1$-2	53.6	17.7	11.0	6.8
$10P_{14}$-2	54.1	21.7	13.2	5.9
$10P_{28}$-2	60.6	16.6	9.4	5.1

References:

1 M. Dounya, U. Maschke, N. Bouchikhi, H. Ziani Chérif and L. Bedjaoui-Alachaher, *Polym. Bull.*, 2023, **80**, 10073–10098.
2 J. Wu, C. Wang, Y. Xiao, C. Mu and W. Lin, *Progress in Organic Coatings*, 2020, **147**, 105812.
3 Q. Tang, X. Sun, Q. Li, J. Lin and J. Wu, *J Mater Sci*, 2009, **44**, 3712–3718.
4 M. Ye, D. Zhang, L. Han, J. Tejada and C. Ortiz, *Soft Matter*, 2006, **2**, 243–256.